Chapter 10
Advanced Experimental and Numerical Analysis of Behavior Structural Materials Including Dynamic Conditions of Fracture for Needs of Designing Protective Structures

Michal Grazka, Leopold Kruszka, Wojciech Mocko, and Maciej Klosak

Abstract The article presents the discussion of modern experimental and numerical techniques used to the design critical infrastructure protection structures. The article presents also the results of experimental researches on S235 steel sheet. The S235 steel sheets were tested using the Hopkinson Bar Technic and perforation tests. In researches were used 3D scanners and numerical controlled measuring machine for checking the final shape after the deformation. The article also presents the results of FEM analysis made using explicit solver. Full-scale CAD model was used in numeric calculations.

Keywords Steel perforation · Ballistic · FEM analysis · CNC measuring

10.1 Critical Infrastructures

Critical infrastructures, the meaning of these words takes on a new look in the era of commonly observed acts of terrorism. Critical infrastructure [1] is a term for describing the resources that are essential for the functioning of society and the economy.

Usually, the critical infrastructure is used for describing:

M. Grazka (✉) · L. Kruszka
Military University of Technology, Warsaw, Poland
e-mail: michal.grazka@wat.edu.pl

W. Mocko
Motor Transport Institution, Warsaw, Poland

M. Klosak
Technical University, Universiapolis, Agadir, Morocco

L. Hofreiter et al. (eds.), *Soft Target Protection*, NATO Science for Peace and Security Series C: Environmental Security,
https://doi.org/10.1007/978-94-024-1755-5_10

- the production, transmission and distribution of electricity (energy),
- the production, transport and distribution of gaseous fuels,
- the production, transport and distribution of crude oil and petroleum products,
- telecommunications (electronic communication),
- water management (drinking water, sewage, surface water),
- the production and distribution of food,
- heating (fuel, heating plant),
- health care (hospitals),
- transport (roads, railways, airports, ports),
- financial institutions (banks); measures,
- security services (police, army, rescue).

Those elements are important and necessary for correct the countries functioning. Therefore, in the times of common acts of terrorism, it is necessary to introduce appropriate policies and systems to protect this infrastructure from damage or destruction. Many countries of the European Union [2] or NATO organization are currently introducing common programs for critical infrastructure protection. More about the protection of critical infrastructure in individual countries is described here [3–5].

One of the easiest ways for protect the critical infrastructure is using the correct building material. These materials connected with correct safety system used in buildings, guaranties good level of protection, the technical principles are described in [6].

10.1.1 Critical Infrastructures – Systems of Building Protection

In critical infrastructure buildings, we often observe many types of protective systems. You can meet in these buildings, for example:

- Special fire protection systems that protect against fire, but also allow smoke removal or safe evacuation of people inside (Fig. 10.1):

- Special systems for registering entrances and exits to the building [7] (Fig. 10.2):

- Special curtain and protection against undesirable intrusion into the confined space (Fig. 10.3)

All of these systems support the protection of critical infrastructure buildings, but do this not in 100%. The critical infrastructure buildings for better protection often were built from special material with dual purpose. One of such materials is a glass,

Fig. 10.1 Fire protection system for modern buildings [2]

Fig. 10.2 In/Out control systems

which, apart from aesthetic functions in building facades [8], is often reinforced to increase the protective capacity of shock waves caused by explosion or penetration by foreign bodies like a projectile (Fig. 10.4).

The laboratory experiments results presented in article focused on another type of material commonly used in construction. This material is steel S235. Steel S235 is widely used in construction. Because this material is very popular in use, it is important to have basic information on the protective capabilities for this steel. In laboratory tests and computer calculations using the FEM method authors of this paper were tested steel S235, dynamic test of this type of steel was tested in [9]. They want to check the protection parameters of this steel.

Fig. 10.3 Unauthorized entering protection system

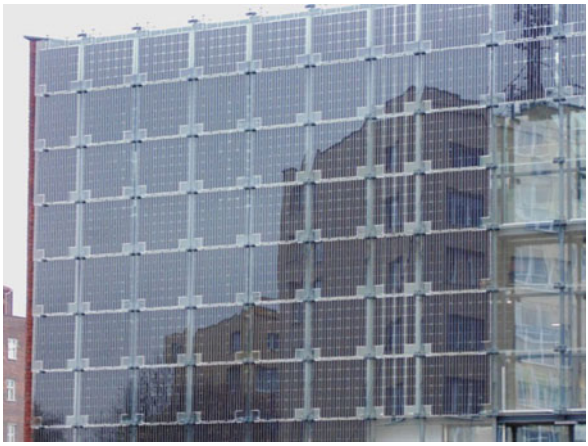

Fig. 10.4 Building glass front wall

10.2 Laboratory Set Up and Experiment Data

10.2.1 Laboratory Infrastructure Description

Laboratory tests of S235 steel sheet and numerical calculations of the dynamic perforation of this sheet were made on a measuring apparatus available in various

Table 10.1 Chemical composition of structural steel S235 [10]

Chemical composites	C [%]	Mn [%]	P [%]	S [%]	Si [%]
Steel S235	0.22	1.60	0.05	0.05	0.05

Table 10.2 Steel S235 yield strength [10]

	Minimum yield strength at nominal thickness 16 mm	
Structural steel	ksi	MPa
S235	33,000	235

Table 10.3 Steel S235 tensile strength [10]

Structural steel	Tensile strength MPa at nominal thickness between 3 mm and 16 mm
S235	360–510 MPa

research centers. Laboratory tests were performed in three different centers. Sheet metal perforation tests were performed in the dynamic research laboratory at the University of Agadir (Morocco). The material properties tests of this steel were made at the Motor Transport Institute, and the measurements of deformation after the laboratory test and numerical calculations using the FEM method were made at the Institute of Armament at the Military University of Technology. The structural steel S235 (ISO standard) or A283C (ASME standard) was used in tests. This steel according to description standards belongs to general purpose construction steels.

The chemical composition of structural steel is extremely important and highly regulated. It is a fundamental factor which defines the mechanical properties of the steel material. In the following Table 10.1 you can see the max % levels of certain regulated elements present in European Structural steel grades S235.

The Mechanical Properties of Structural Steel are fundamental to its classification and hence, application. Even though Chemical Composition is a dominant Factor of the Mechanical Properties of steel, it is also very important to understand the minimum standards for the Mechanical Properties.

The yield strength of structural steel measures the minimum force required to create a permanent deformation in the steel. The naming convention used in European Standard EN10025 refers to the Minimum Yield strength of the steel grade tested at 16 mm thick (Table 10.2).

The Tensile Strength of Structural steel relates to the point at which permanent deformation occurs when the material is pulled or stretched laterally along its length (Table 10.3).

Square steel sheet samples with dimensions 130 mm × 130 mm with two different thicknesses were used during the laboratory tests. The sheets thickness was 0.6 mm and 1.0 mm. The perforation laboratory tests were made on square steel sheets. Pneumatic gun was used during this laboratory tests [11]. The cylindrical steel projectiles with a diameter 12.7 mm and a conical tip with the approximately

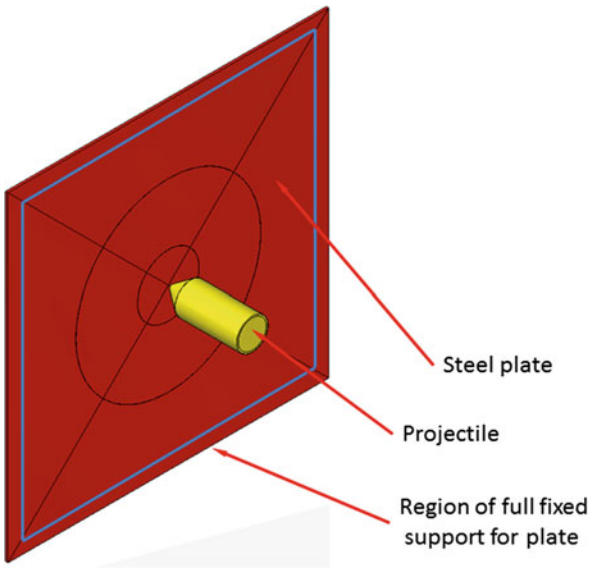

Fig. 10.5 Plate-projectile configuration during the laboratory experiments

Fig. 10.6 Hopkinson Pressure Bar set-up for investigation of dynamic behavior of material [12]

weighing 28 g were used. These tests were carried out for two temperatures: room temperature (20 °C) and higher temperature (300 °C). The plates were mounted on the circumference (Fig. 10.5) so that they could not be displaced during the perforation by the projectile.

The dynamic properties of S235 steel was obtained by the Split Hopkinson Tensile Bar [12–15] tests (Fig. 10.6). Similarly, the fatigue from thy dynamical

Fig. 10.7 CNC measuring machine used for plate deformation calculation [12]

loading was researched in [16, 17]. The deformation of steel sample after the perforation in ballistic tests was measured using the coordinate measuring machines (Fig. 10.7).

10.2.2 Results of Laboratory Experiments

The perforation laboratory tests were carried out for two types of steel sheet thicknesses. The projectile impact speed was changed in range 0 up to 120 m/s and the tests were in two temperatures. Figure 10.8 shows the final sample shapes with the hole after the perforation.

During the tests, the initial velocity (v_0) of the projectile was measured at the moment of impact on the steel sheet and residual velocity (v_R) after the perforation. The results of these measurements are shown in Table 10.4.

The steel sheets after the laboratory tests were analyzed. The final shape and the figure of perforation holes were checked. In each of the described cases (Table 10.4), characteristics 4 petals were observed, on perforation region (Fig. 10.9).

In the next analysis step, the value of deformation on the surface of the steel sheets was measured. The measurements were made using a CNC measuring machine [1]. The results of these measurements were presented using 3D plots (Fig. 10.10).

The thickness of the steel sheet and the projectile impact velocity has influence on the final shape after the perforation. Normal shape which we expected to get is one side convex (positive deformation) (Fig. 10.10a, b). But the steel sheets which were in temperature 300 °C the final shape is different. The steel samples have positive

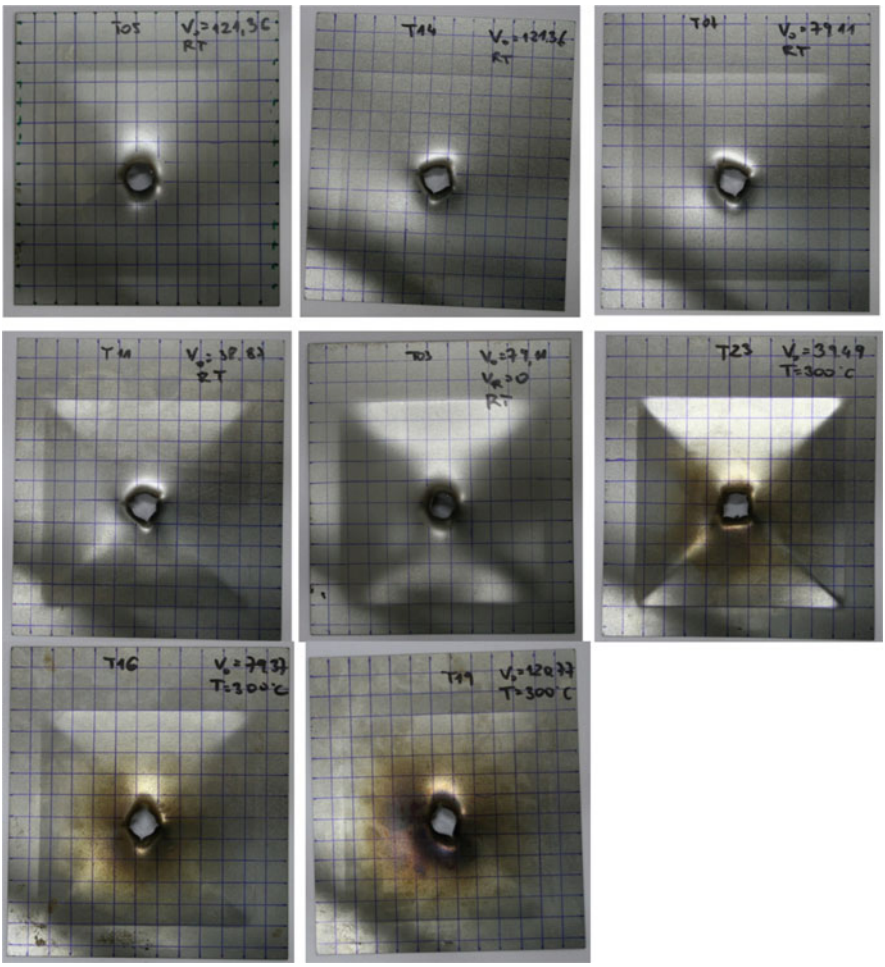

Fig. 10.8 Final results of ballistic experiments

and negative deformation (Fig. 10.10e, f). In these causes the temperature generates internal stresses which are observed on these samples. The maximum of deformation observed during the tests is 4 mm. The information about value of deformation was useful on next step of investigation. This information was use to validation results of numerical calculation.

10.2.3 Kinetic Energy Calculation

In laboratory test we record the impact speed and the residual speed of projectile. The information of projectile speed before and after perforation is useful for kinetic

Table 10.4 Velocity of impact and residual velocity of each ballistic test

Test no	Pressure (bar)	Temperature [C]	Impact velocity V0 (m/s)	Time (ms)	Residual velocity (m/s)
Steel thickness 0.6 mm					
T10	1.0	20	44.17	2.480	20.16
T9	1.5	20	54.11	1.440	34.72
T8	2.0	20	64.43	1.080	46.30
T7	3.0	20	79.11	0.740	67.57
T12	4.0	20	90.58	0.640	78.13
T13	5.0	20	100.40	0.540	92.59
T14	7.5	20	121.36	0.440	113.64
T23	0.8	300	39.49	4960	10.08
T22	1.0	300	43.55	2.100	23.81
T21	1.5	300	55.93	1.190	42.02
T20	2.0	300	64.60	0.890	56.18
T16	3.0	300	79.37	0.660	75.76
T17	4.0	300	90.91	0.570	87.72
T18	5.0	300	100.81	0.490	102.04
T19	7.5	300	120.77	0.430	116.28
Steel thickness 1.0 mm					
T2	2.0	20	64.93	–	0.00
T3	3.0	20	79.11	0.000	0,00
T6	3.2	20	83.06	2.400	20.83
T1	4.0	20	90.25	1.000	50.00
T4	5,0	20	101.21	0.780	64.10
T5	7.5	20	121.36	0.540	92.59
T24	2,7	300	75.50	0.000	0.00
T25	3.0	300	79.11	1.440	34.72
T26	4.0	300	91.24	0.830	60.24
T27	5.0	300	101.62	0.660	75.76
T28	7.5	300	122.55	0.490	102.04

energy calculation. Information about kinetic energy changing during the perforation, inform us about possibility to energy dissipation on material in dynamic load. Figures 10.11 and 10.12 show graphs with information about percentage change in kinetic energy of a projectile during penetration of a steel sheet.

The graphs on Figs. 10.11 and 10.12 show the kinetic energy changes. There is compered information about projectile kinetic energy changes after the perforation in steel sheet in temperature 20 °C and 300 °C. According to the information on graphs (Figs. 10.11 and 10.12), higher temperature decreases the protective capacity of S235 steel sheet. For temperature differences about 280 °C this protective capacity is lower around 5%. Also the thickness of the steel sheet is important on the protective capacity. Big thickness guaranties better protection abilities. How can we observe in Figs. 10.11 and 10.12 the total differences in kinetic energy recorded for 1.0 mm and 0.6 mm steel sheets is 14% higher for the 1.0 mm samples.

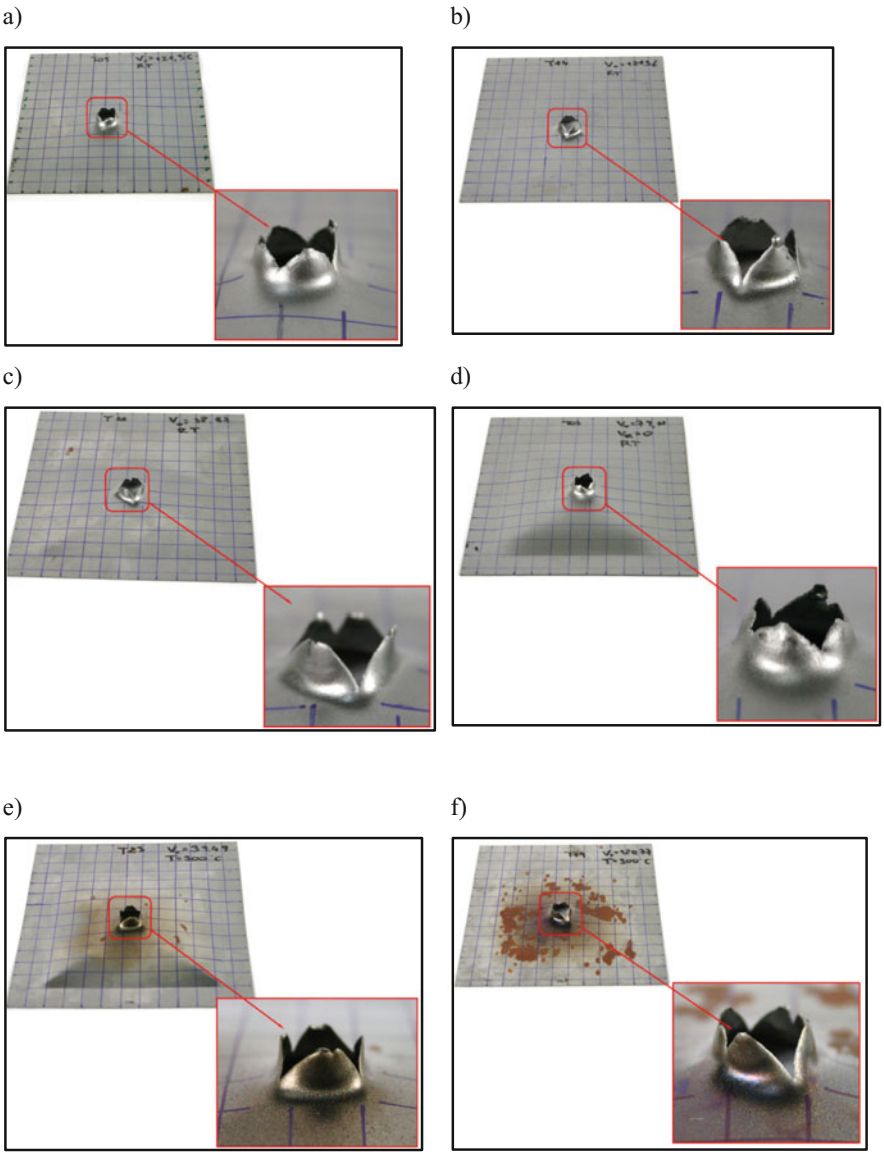

Fig. 10.9 Comparison the shape of penetration region for each tests

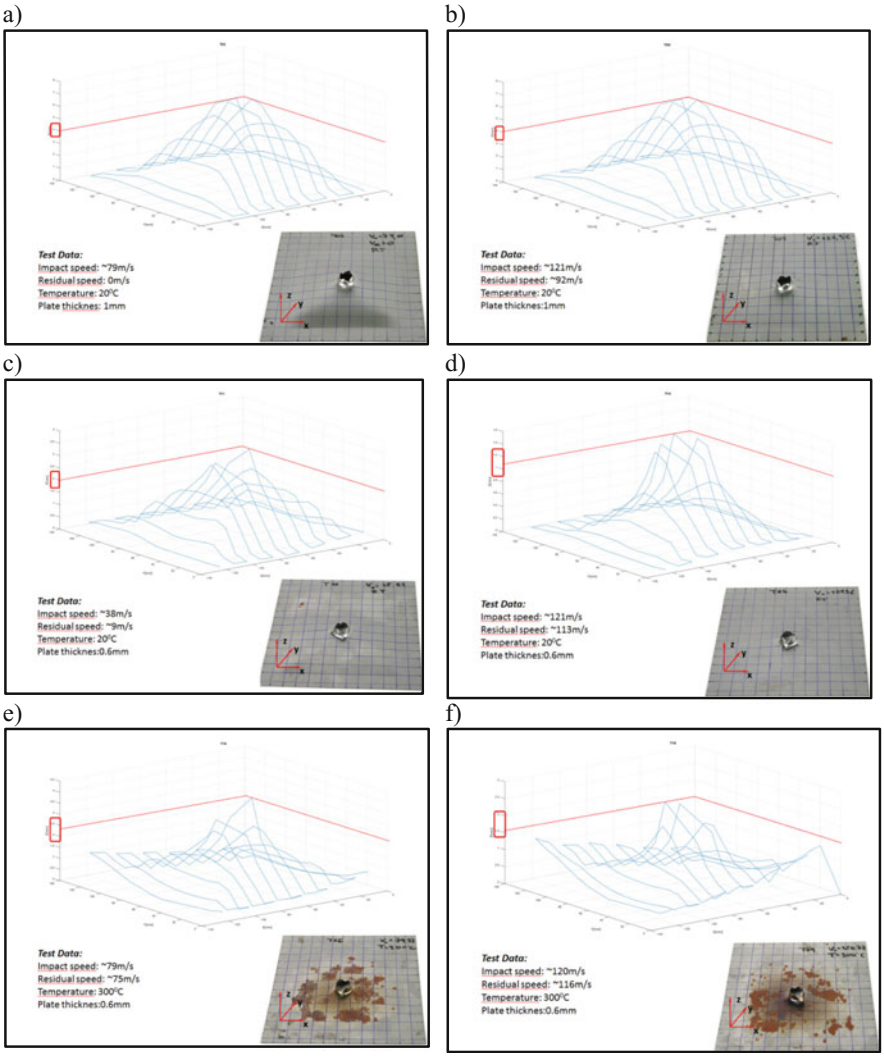

Fig. 10.10 Plate shape (deformation) after the ballistic tests

10.3 Numeric Calculation Using FEM Method

10.3.1 Numeric Simulation – Initial and Boundary Conditions

Numerical calculations were done using Ansys Workbench software [13]. Calculations were calculated in explicit solver. In the calculations full CAD models of S235 steel sheet and projectile were used (Fig. 10.13).

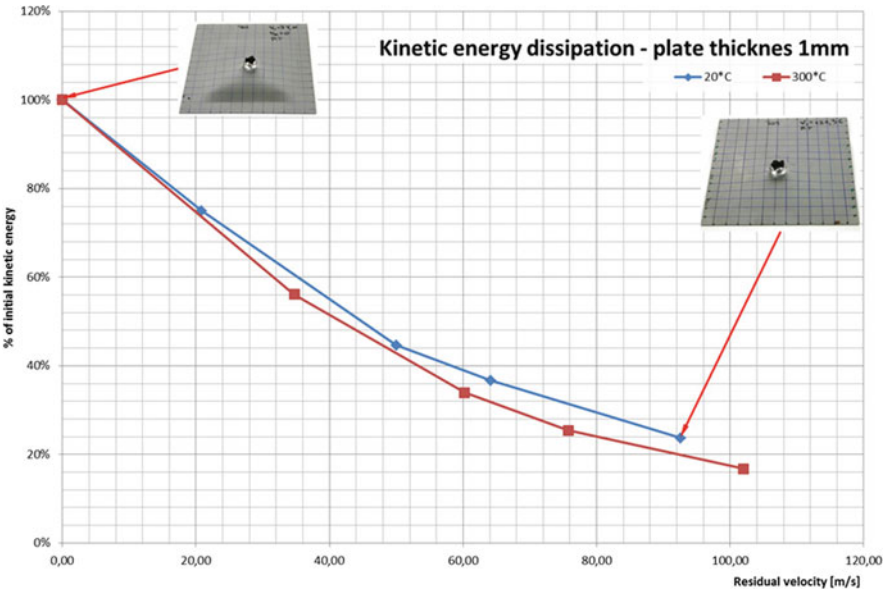

Fig. 10.11 Kinetic energy dissipation on 1.0 mm thickness steel plate

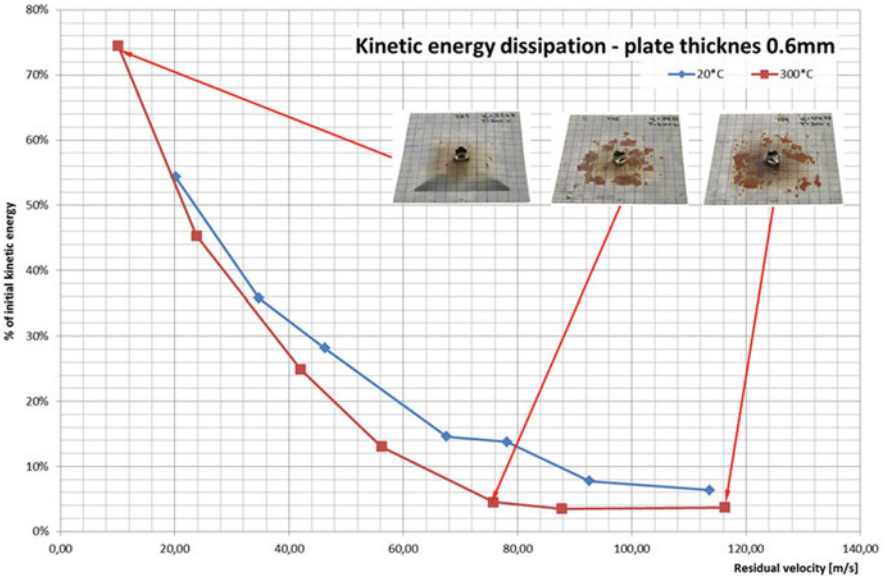

Fig. 10.12 Kinetic energy dissipation on 0.6 mm thickness steel plate

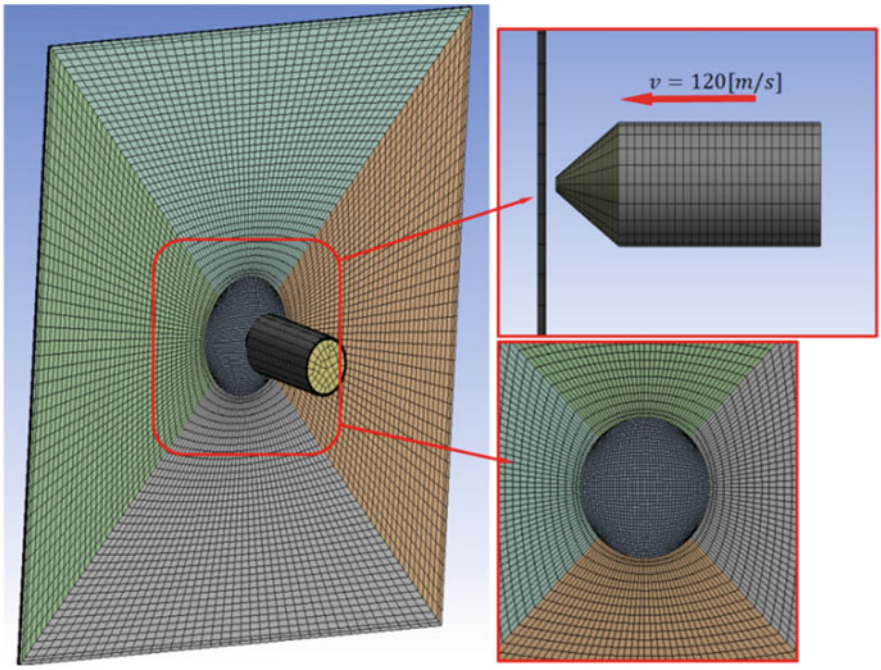

Fig. 10.13 3D cad model of steel plate and projectile used in numeric calculation

During the computer calculations the steel sheets were fixed in the same way as used in the laboratory tests (Fig. 10.14).

The explicit solver was used in the numeric calculations. This type of solver is dedicated for high speed material deformation. This calculation need to use specialist material models for good correctness between laboratory and numerical calculation results. The Johnson-Cook [13, 15] constitutive material model was used for describing the dynamic material behavior of S235 steel. The Johnson-Cook constitutive constants were approximated using data from static and dynamic tensile test. The static tests were done using MTS tensile testing machine. The dynamic tests were done using the Split Tensile Hopkinson Bar equipment. Figure 10.15 shows the stress-strain curves for 600 1/s deformation speed. In tests were used dedicated for this kind tests samples. They were flat samples.

The constants of Johnson-Cook constitutive model accepted for calculation were: A-280 MPa, B-667 MPa, n-0.72, C-0.071. The "m" parameter was omitted in computer calculation of perforation the steel sheet. There were no tests in lower and higher temperatures which are important in calculation this parameter.

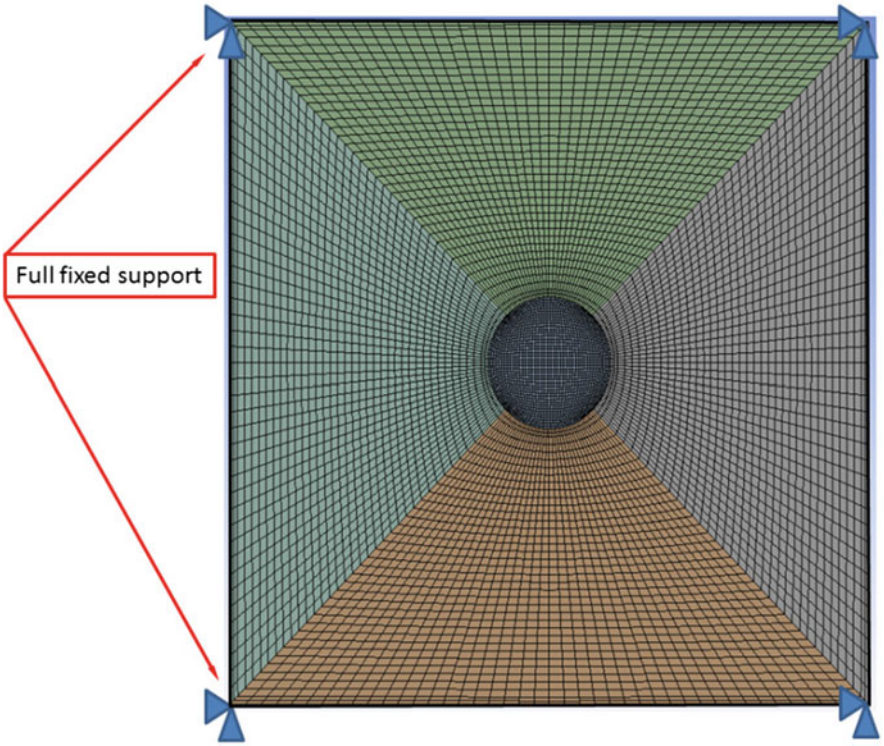

Fig. 10.14 Full fixed support used on external edges of steel plate

Fig. 10.15 True stress-strain curve

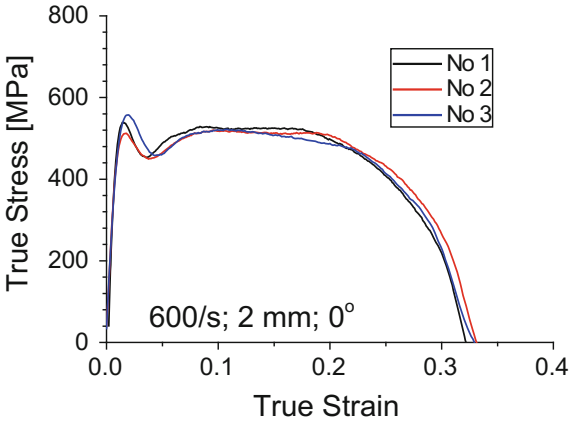

10.3.2 Numeric Simulation – Results

The computer calculations were made to get the perforation data. The results on numerical calculations were compared with laboratory test data. Figure 10.16a, b show final shapes of steel sheet after perforation and numerical calculations.

In both cases (numeric calculation, laboratory test), we observe the same characteristic 4 petals in region where was perforation. The final shape of steel plates was also same. The results of the computer simulation were also used to analyze the kinetic energy dissipation during the perforation the steel sheet. The results of computer calculations were compared with laboratory test data. Information about this comparison is presented on Fig. 10.17.

The results of dissipation the kinetic energy are presented on Fig. 10.17. The results of laboratory tests and computer calculations by FEM methods were compared. For steel sheet with thickness 0.6 mm, we observed the good correlation between results calculated by FEM method and from laboratory experiments.

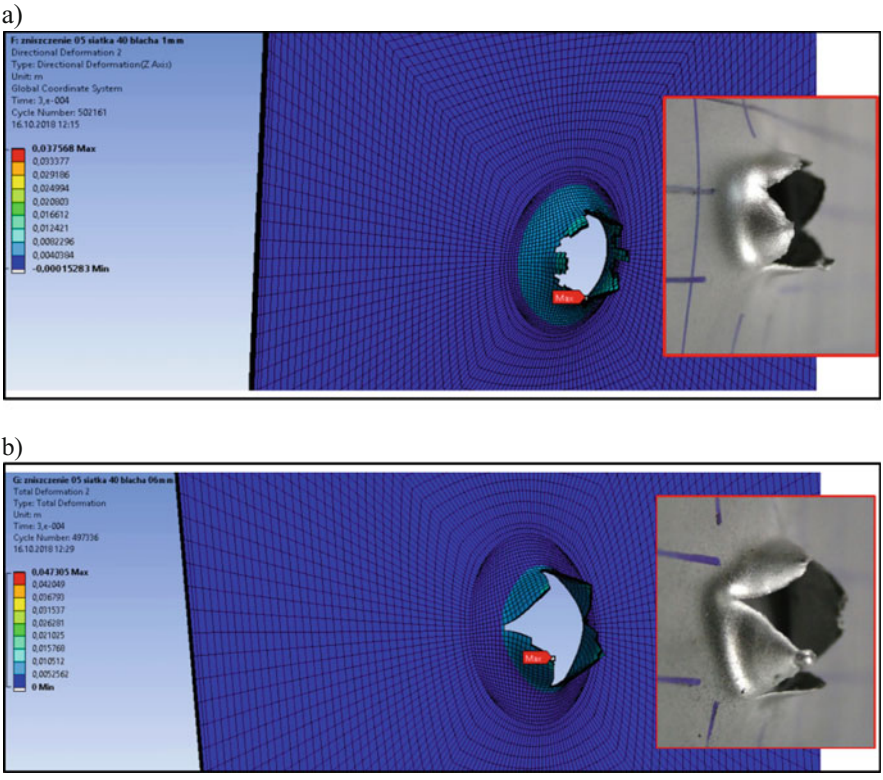

Fig. 10.16 Deformation and perforation regions - comparison

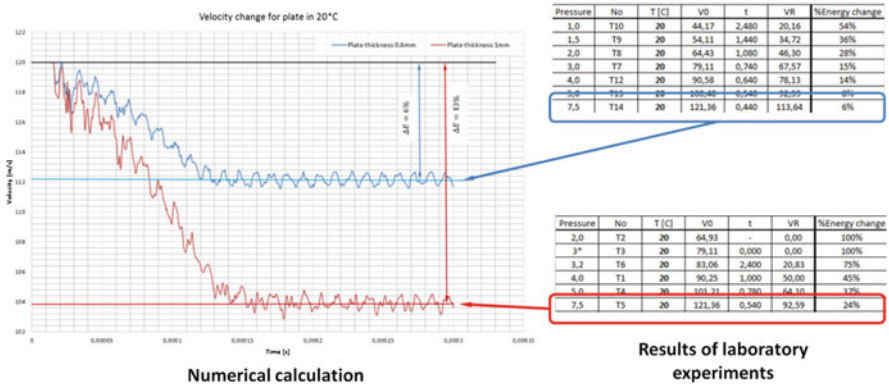

Pressure	No	T [C]	V0	t	VR	%Energy change
1,0	T10	20	44,17	2,480	20,16	54%
1,5	T9	20	54,11	1,440	34,72	36%
2,0	T8	20	64,43	1,080	46,30	28%
3,0	T7	20	79,11	0,740	67,57	15%
4,0	T12	20	90,58	0,640	78,13	14%
5,0	T15	20	100,40	0,540	92,59	8%
7,5	T14	20	121,36	0,440	113,64	6%

Pressure	No	T [C]	V0	t	VR	%Energy change
2,0	T2	20	64,93	-	0,00	100%
3*	T3	20	79,11	0,000	0,00	100%
3,2	T6	20	83,06	2,400	20,83	75%
4,0	T1	20	90,25	1,000	50,00	45%
5,0	T4	20	101,21	0,780	64,10	37%
7,5	T5	20	121,36	0,540	92,59	24%

Fig. 10.17 Kinetic energy dissipation observed in numerical model and laboratory tests

For steel sheets with thickness 1.0 mm the correlation between FEM method calculation and laboratory experiments is much bigger. Kinetic energy dissipation calculated by FEM methods is 13% and data from laboratory experiments shows the dissipation on 24%.

10.4 Summary

The article presents the results of laboratory tests and numerical calculations by FEM methods. During the tests the S235 steel sheets were tested. In these teste protective capacity on dynamic load was checked. For investigation were used modern measuring techniques. During the test Split Hopkinson Bar, Coordinate Measuring Machines and FEM analysis were used. Results of these experiments were presented in this paper.

The presented results as well as the methodology of conduct are important elements of the design of building panels, protective divisions of critical infrastructure facilities made of steel sheets related to determining the resistance of these panels to perforation in the conditions of fires.

References

1. PWN (2018) Great Polish dictionary
2. Council Directive 2008/114/EC of 8 December 2008 on the identification and designation of European critical infrastructures and the assessment of the need to improve their protection, European Union (2008)
3. Sventekova E, Leitner B, Dvorak Z (2017) Transport critical infrastructure in Slovak republic. In: IMCIC 2017 – 8th International Multi-Conference on Complexity, Informatics and Cybernetics, Proceedings 2017-March, pp 212–215

4. Leitner B, Môcová L, Hromada M (2017) A new approach to identification of critical elements in railway infrastructure. Process Eng 187:143–149
5. Figuli L, Kavický V, Picot S (2017) Analysis of the different approaches to protection of critical infrastructures in France and Slovakia. In: Lecture notes in mechanical engineering PartF11. American Society of Mechanical Engineers, New York, pp 120–128
6. Manas P (2017) The protection of critical infrastructure objects – technical principles. In: Lecture notes in mechanical engineering PartF11. American Society of Mechanical Engineers, New York, pp 239–248
7. Loveček T, Velas A, Kampová K, Mariš L, Mózer V (2013) Cumulative probability of detecting an intruder by alarm systems. In: Proceedings – International Carnahan Conference on Security Technology
8. Bedon C, Zhang X, Santos F, Honfi D, Kozłowski M, Arrigoni M, Figuli L, Lange D (2018) Performance of structural glass facades under extreme loads – design methods, existing research, current issues and trends. Constr Build Mater 163:921–937
9. Figuli L, Jangl Š, Papán D (2016) Modelling and testing of blast effect on the structures. IOP Conf Ser Earth Environ Sci 44(5):052051
10. European Standard EN10025:2004 (2004)
11. Klosak M, Rusinek A, Bendarma A, Jankowiak T, Lodygowski T (2017) Experimental study of brass properties through perforation test using a thermal chamber for elevated temperatures. Latin Am J Solid Struct. https://doi.org/10.1590/1679-78254346
12. Moćko W, Janiszewski J, Radziejewska J, Grazka M (2015) Analysis of deformation history and damage initiation for 6082-T6 aluminium alloy loaded at classic and symmetric Taylor impact test conditions. Int J Impact Eng 75:203–213
13. Grazka M, Janiszewski J (2012) Identification of Johnson-Cook equation constants using finite element method. Eng Trans 60(3):215–223
14. Panowicz R, Janiszewski J, Kochanowski K (2017) The influence of non-axisymmetric pulse shaper position on SHPB experimental data. J Theo Appl Mech (Poland) 56(3):873–886
15. Kruszka L, Janiszewski J (2015) Experimental analysis and constitutive modelling of steel of A-IIIN strength class. EPJ Web Conf 94:05007
16. Leitner B, Lusková M, Dvořák Z, Sventekova E (2017) Fatigue damage prediction as a part of technical systems reliability assessment. Key Eng Mater 755:131–138
17. Leitner B, Figuli L (2017) Fatigue life prediction of mechanical structures under stochastic loading. In: MATEC Web of Conferences, vol. 157, 22nd Slovak-Polish Scientific Conference on Machine Modelling and Simulations, MMS 2017